Available online at www.sciencedirect.com
ScienceDirect
Physica D 223 (2006) 26–35
PHYSICA D
www.elsevier.com/locate/physd

Dynamics of infectious diseases and pulse vaccination: Teasing apart the embedded resonance effects

Marc Choisy[a,*], Jean-François Guégan[b], Pejman Rohani[a]

[a] *Institute of Ecology, University of Georgia, Athens, GA 30602-2202, USA*
[b] *GEMI, UMR CNRS-IRD 2724, Centre IRD, 911 avenue Agropolis BP 64501, 34394 Montpelier Cedex 5, France*

Received 16 December 2005; received in revised form 7 June 2006; accepted 8 August 2006
Available online 9 October 2006
Communicated by A. Doelman

Abstract

Dynamical systems theory predicts that inherently oscillatory systems undergoing periodic forcings will exhibit resonance phenomena, which are characterized by qualitative dynamical consequences resulting from the amplification of small external perturbations. In this paper we use extensive numerical simulations to demonstrate that the periodic nature of pulse vaccination strategies can make disease dynamics resonate. We proceed step by step in order to tease apart the dynamical consequences of (i) the intrinsic nonlinearity of the host–pathogen system, (ii) the seasonal variation in transmission and (iii) the additional forcing caused by vaccinating in pulses. We document that the resonance phenomenon associated with pulse vaccination can have quantitative epidemiological implications and produce perverse effects such as an unexpected increase in the number of infectives as the vaccination frequency increases. Our findings emphasize the importance of carefully taking into account the dynamical properties of the disease when designing a pulse vaccination strategy.

Keywords: Infectious diseases; Population dynamics; Parametric resonance; Environmental forcing; Pulse vaccination

1. Introduction

The dynamics of most directly transmitted childhood diseases are characterized by pronounced oscillations, with alternating "boom" (epidemic, outbreak) and "bust" (inter-epidemic) periods [3,28,38,17,24]. This observation has motivated an impressive number of studies, ranging from the theoretical to the applied perspective. Ecologically, the most commonly addressed questions concern infection persistence [7,11,31,39], spatial synchrony of epidemics [6,12,34,18,38, 25], and the impact of vaccination [3,49,28,13,17,25,40]. From a more theoretical point of view, there have been a number of investigations into the complex and nonlinear nature of epidemiological systems [41,10,37,19,50,32,8]. A particularly interesting area has been to develop an understanding of the interaction between the weakly damped oscillations of epidemic systems and external forcing (e.g., the school year cycle), which can give rise to a plethora of complex patterns, such as a cascade of period-doubling bifurcations and chaos [15,26,43,22]. Surprisingly, the phenomenon of resonance, i.e. the excitation of oscillations by external forcing, has received little attention by epidemiologists and ecologists. This is all the more surprising given the numerous potential sources of resonance in such systems and their possible dynamical consequences both in qualitative and quantitative terms (see, for example, [50]). A recent exception is the work of Greenman et al. [23], who showed that resonance has great potential for shedding light on the dynamics of ecological and epidemiological systems. In this paper, we explore resonance phenomena in models of disease transmission. We begin by studying the resonance associated with seasonality in transmission (as due to the alternation of holidays and school terms). In a second stage we focus on the resonance related to the periodic nature of pulse vaccination, first without and then together with seasonality in transmission.

The rationale underpinning classical vaccination policy is to ensure the proportion of susceptible individuals in the

* Corresponding author. Tel.: +1 706 542 5380; fax: +1 706 542 5380.
E-mail address: choisy@uga.edu (M. Choisy).

0167-2789/$ - see front matter © 2006 Elsevier B.V. All rights reserved.
doi:10.1016/j.physd.2006.08.006

population remains below the threshold necessary for an epidemic [4]. The most commonly used scheme for the control of childhood microparasitic infections is called paediatric mass vaccination. It is based on the static properties of the host–pathogen system and involves vaccinating a critical fraction of infants before they reach a specific age cohort, usually 0–2 years [4]. An alternative and potentially less expensive strategy, called pulse vaccination, has been recently proposed [2,36]. This scheme explicitly accounts for the host population dynamics and involves the periodic immunization of a specified proportion of the susceptible population to prevent invasion of the infection. A number of elegant studies have determined the optimal vaccination coverage and frequency to eradicate common infections, such as measles [2,45,16]. Interestingly, d'Onofrio [16] briefly mentioned the potential for "parametric resonance" (defined below) resulting from the periodic nature of vaccination pulses. However the dynamical consequences of such a resonance phenomenon have never been studied in detail. Moreover, the models exploring periodic vaccination have ignored so far the well-documented seasonality in disease transmission (primarily to facilitate analytical tractability).

The present work addresses this problem through extensive numerical simulations to study in detail the resonance-induced quantitative consequences of pulse vaccination in a context of seasonally varying disease transmission. Given the potential for complex dynamics, we proceed step by step in order to tease apart the consequences of interactions between the inherent nonlinearity of these systems and different external forcings (seasonality and vaccination pulses). We first review the classical *SEIR* model, highlighting the source of nonlinearity. We then introduce sinusoidal variation in disease transmission (to mimic the alternation of school terms and holidays). Within this simple set-up, we provide a description of the different characteristics of resonance, both linear and nonlinear, and contrast the quantitative predictions of resonance due to seasonality in disease transmission with the patterns observed in epidemiological data. We finally incorporate pulse vaccination into the model. Despite the increased degree of complexity in the dynamics, parametric resonance associated with the periodic vaccination pulses is clearly identified. We focus on its quantitative epidemiological consequences, in terms of incidence, and reveal potential counter-intuitive effects such as an increased number of infectives as the frequency of vaccination rises. The results of this study have strong implications for the design of pulse vaccination schemes and these are discussed at the end of the paper.

2. The model

Consider the propagation of an immunizing, non-fatal, acute disease in a constant population of N individuals. The dynamics of diseases, such as childhood diseases, characterised by a substantial period of asymptomatic latency following infection can be modeled using the classical *SEIR* framework [15,4,14] where the dynamics of the susceptible (S), infected but not infectious (E), infectious (I), and recovered (R) individuals are described by the following differential equations:

$$\frac{\mathrm{d}S}{\mathrm{d}t} = \mu N - (\lambda + \mu)\, S \tag{1}$$

$$\frac{\mathrm{d}E}{\mathrm{d}t} = \lambda S - (\sigma + \mu)\, E \tag{2}$$

$$\frac{\mathrm{d}I}{\mathrm{d}t} = \sigma E - (\gamma + \mu)\, I \tag{3}$$

$$\frac{\mathrm{d}R}{\mathrm{d}t} = \gamma I - \mu R \tag{4}$$

where μ is the population turn-over rate, λ is the force of infection (the per capita rate of acquisition of infection) and $1/\sigma$ and $1/\gamma$ are the mean latent and infectious periods, respectively. Note that the host population turn-over rate is equal to both the birth and the death rates. The consequence of this assumption is that high birth rates imply short life expectancy and low birth rates imply long life expectancy. In the case of childhood diseases, this is not a problem for two reasons. First, human populations are actually characterised by a negative relationship between the birth rate and the life expectancy, with developing countries generally characterised by high birth rates and short life expectancy, and developed countries more characterised by low birth rates and long life expectancy. Second, in the case of childhood diseases, where the mean age at infection is low and the acquired immunity is life-long, we are not really concerned about the life expectancy, only the birth rate really matters.

Here, the force of infection is modelled as proportional to the infection prevalence: $\lambda = \beta I$, as usually assumed for directly transmitted infections (such as measles, whooping cough, influenza, etc.) [15]. The proportionality constant β reflects the contact rate. The basic reproduction ratio R_0, defined as the average number of secondary infections produced by one infected individual introduced into a fully susceptible population [4], is expressed as

$$R_0 = \frac{\beta N \sigma}{(\gamma + \mu)\,(\sigma + \mu)}. \tag{5}$$

Note that for most childhood diseases like measles or whooping cough, $\gamma \gg \mu$ and $\sigma \gg \mu$ making R_0 approximately independent of μ.

The system of Eqs. (1)–(4) possesses two equilibria (the disease-free and the endemic), the stability of which depends solely on R_0. If R_0 is less than unity, then the disease-free equilibrium is stable, while $R_0 > 1$ means the endemic equilibrium is stable. Perturbations to the endemic equilibrium result in damped oscillations before the equilibrium is recovered. Linear stability analysis reveals the natural period T and the damping time T_D of this system to be approximated by

$$\widehat{T} = 2\pi\sqrt{AG} \tag{6}$$

and

$$\widehat{T_D} = 2A \tag{7}$$

respectively, where A represents the mean age at infection, $A \simeq 1/\mu(R_0 - 1)$, and G gives the ecological generation length of the infection, i.e. the sum of latent and infectious periods, $G = [1/(\mu + \gamma)] + [1/(\mu + \sigma)]$ [4,40]. For most epidemiologically reasonable parameter values, the damping time is typically much longer than the natural period: $\widehat{T_D} \gg \widehat{T}$. This renders the endemic equilibrium weakly stable, with relatively small perturbations (intrinsic or extrinsic) "exciting" the inherent oscillatory behavior [26] and thus generating sustained oscillations as observed on the dynamics of most childhood diseases [35,20,3,21,28,38,17,24].

In this paper, the inherent oscillations of our system are excited by a sinusoidal forcing on the contact rate β, intended to reflect the alternation of school terms and holidays [35,20, 42,21,4]:

$$\beta(t) = \beta_0 \left(1 + \beta_1 \cos\left(\frac{2\pi}{T_S} t\right)\right), \quad 0 \leqslant \beta_1 < 1. \tag{8}$$

The strength of seasonality β_1 measures the amplitude of the oscillations around the baseline coefficient of transmission β_0, and T_S is the period of forcing. For childhood diseases, $T_S = 1$. However, since we are interested in the value of T_S relative to the natural period T, instead of studying different combinations of the epidemiological parameters β_0, σ, and γ, our approach is to keep T constant and vary T_S [23]. Thus, in the simulations presented in the next section, we will take classically estimated measles values ($\beta_0 = 0.0002$ yr^{-1} · individual^{-1}, $\sigma^{-1} =$ 7.5 day, and $\gamma^{-1} = 6.5$ day; [4]) and let T_S vary from 0.1 to 10 yr. The population size will be fixed at $N = 5 \times 10^6$ individuals, yielding an R_0 around 17.

3. Non-linearity and exploration process

The nonlinearity of a dynamical system is often the source of complexity in the dynamics. Within the context of the *SEIR* system, the sole source of nonlinearity is density dependence in the transmission process (represented by the bilinear term βIS). For a sufficiently large rate of susceptible recruitment, μ, the μN term in Eq. (1) dominates and the transmission term can essentially be considered linear. In order to derive the approximate value of μ for which this is true, we wish to ensure that $\frac{dI}{dt} > 0$. This condition will be approximately satisfied if the minimum number of susceptibles exceeds N/R_0 [33]. Therefore, we obtain an expression for S by setting Eq. (1) to zero:

$$S = \frac{\mu N}{\beta I + \mu}. \tag{9}$$

In order to ensure $S > N/R_0$, we must have $\mu > \frac{\beta I}{R_0 - 1}$. Thus, we can obtain a conservative estimate for this criterion by insisting it is satisfied at the peak of the epidemic:

$$\mu_c > \frac{\beta_0(1 + \beta_1)}{R_0 - 1} \max(I). \tag{10}$$

Extensive numerical simulations reveal that, for much of the parameter space, $\max(I) < 10^{-3} N$ [17]. Substituting this, together with the other parameter values used in our simulations, into Eq. (10), we get $\mu_c \simeq 0.07$ yr^{-1}. Consequently, for $\mu > 0.07$ yr^{-1} the linear approximation becomes reasonable. Conversely, the lower the recruitment rate below 0.07, the larger the nonlinear influence and the more complicated dynamics are expected. In practice, the recruitment rate vary from 0.02 in developed countries to 0.05 in developing countries, meaning that nonlinearity of the transmission process is expected to influence the dynamics of the disease. This influence of the recruitment rate on the complexity of the dynamics has been verified in measles dynamics using both simulations and time-series analysis [17,24]. These authors also demonstrated the correspondence between the recruitment rate μ and the mean coefficient of transmission β_0, predicting similar dynamical consequences of increasing μ and increasing β_0. For simplicity, in the following we will vary only μ. We illustrate the dynamical properties of the seasonally forced *SEIR* model (with and without pulse vaccination) by first considering the simple case of approximately linear dynamics (harmonic resonance) observed for large (and rather unrealistic) rates of susceptible recruitment μ (i.e. $0.07 < \mu < 0.10$). We then explore the consequences of nonlinearity (subharmonic and parametric resonance) by progressively decreasing the recruitment rate μ towards realistic values (i.e. $0.01 < \mu < 0.05$).

3.1. Resonance and non-linearity

We now proceed to define some of the basic terminology of resonance phenomena in forced systems. "Resonance" is a generic term that indicates a relationship between the amplitude of observed oscillations and the period of forcing, with a clear maximum. This maximum is called the "resonance peak", with a corresponding "resonance period" (the forcing period at which the resonance peak occurs). The simplest type of resonance – harmonic or linear resonance – arises in the special case where the system can be approximated as linear, i.e. for high values of the population turn-over rate in our model ($\mu > 0.07$, see the previous section). In the more general case where the system is nonlinear (i.e. when μ decreases below 0.07 in our model, see the previous section), we observe more complex types of resonance: subharmonic and parametric resonance. Below, these different kinds of resonance are detailed.

3.2. Linear systems and harmonic resonance

The two fundamental properties of linear systems are that (i) they oscillate sinusoidally, and (ii) their natural period is independent of their amplitude. When periodically excited, linear systems exhibit *harmonic oscillations*, meaning they oscillate with the same period as the forcing, which is not necessarily equal to the natural period. This is because, in some sense, the external forcing is additive [15]. When the forcing period equals the natural period of the unforced system, the amplitude of the oscillations reaches its maximum (i.e. resonance peak). For this type of resonance – called harmonic resonance – there is one unique resonance peak and the resonance period is thus equal to the natural period [29].

For the forced *SEIR* system, this would mean that whenever the period of seasonality T_S equals the natural period T, maxima in the coefficient of transmission ($\beta(t)$) and the number of infectives $I(t)$ coincide, thus amplifying the magnitude of the oscillations. These possibilities are explored in Fig. 1A, which shows a resonance diagram [30] where the peak and trough numbers of infectives are plotted against the logarithm of the forcing period T_S. It demonstrates how, as T_S increases, we observe a dramatic rise (decline) in the peak (trough) number of infectives, with a clear turning point after which the amplitude of oscillations declines. The excellent agreement between this resonance period (resonance peak at $T_S = T \simeq 1.05$ years; Fig. 1A) and the approximate natural period from Eq. (7) (vertical line at $T_S = \widehat{T} \simeq 0.95$ years; Fig. 1A) is confirmation of the linear approximation: $(T - \widehat{T})/T \simeq 0.10$. Indeed, as μ further increases, $T - \widehat{T}$ tends towards 0 (results not shown).

3.3. Nonlinear systems and nonlinear resonances

In the more general case where the system is nonlinear, the above-mentioned two fundamental properties of harmonic oscillators do not hold anymore. Namely, (i) they do not oscillate sinusoidally, and (ii) their natural period becomes dependent of their amplitude. From the first property there results subharmonic resonance where each harmonic of the system can give rise to a resonance peak (see Fig. 1B–D). From the second property there results a fold-over effect where the dependency between the amplitude of the oscillations and the natural period of the system progressively shifts this latter out of the resonance domain as the forcing period increases. This results in these characteristic asymmetric peaks of resonance. When nonlinearity further increases, the period–amplitude relationship accentuates the asymmetry of the peak, bending it further and even folding it over itself (see for example, Fig. 1C at $T_S \simeq 1$ or Fig. 1D where it is even more pronounced). This fold-over effect leads to bistability and hysteresis, i.e. the system oscillations may have either a large or a small amplitude with an unstable periodic solution in between. At the end of the interval of bistability this unstable limit cycle annihilates with one of its stable counterparts in a saddle–node bifurcation.

Focusing only on the peak values of the number of infectives, Fig. 2A illustrates the nonlinear effect of a continuous decrease in μ (from 0.10 to 0.01/person/yr) on the resonance phenomenon.

3.4. Parametric resonance and dependency among parameters

Parametric resonance occurs when one of the parameters (the coefficient of transmission β in our model) is not constant but time-dependent. This type of resonance differs from harmonic and subharmonic resonances in that it is an instability phenomenon stemming from the weak stability of the endemic equilibrium [29]. The fundamental property of parametric resonance is that resonance peaks are expected at integer fractions of the natural period, once a control parameter has exceeded a certain threshold, with each parametric resonance peak having its own threshold value. Grossman et al. [27]

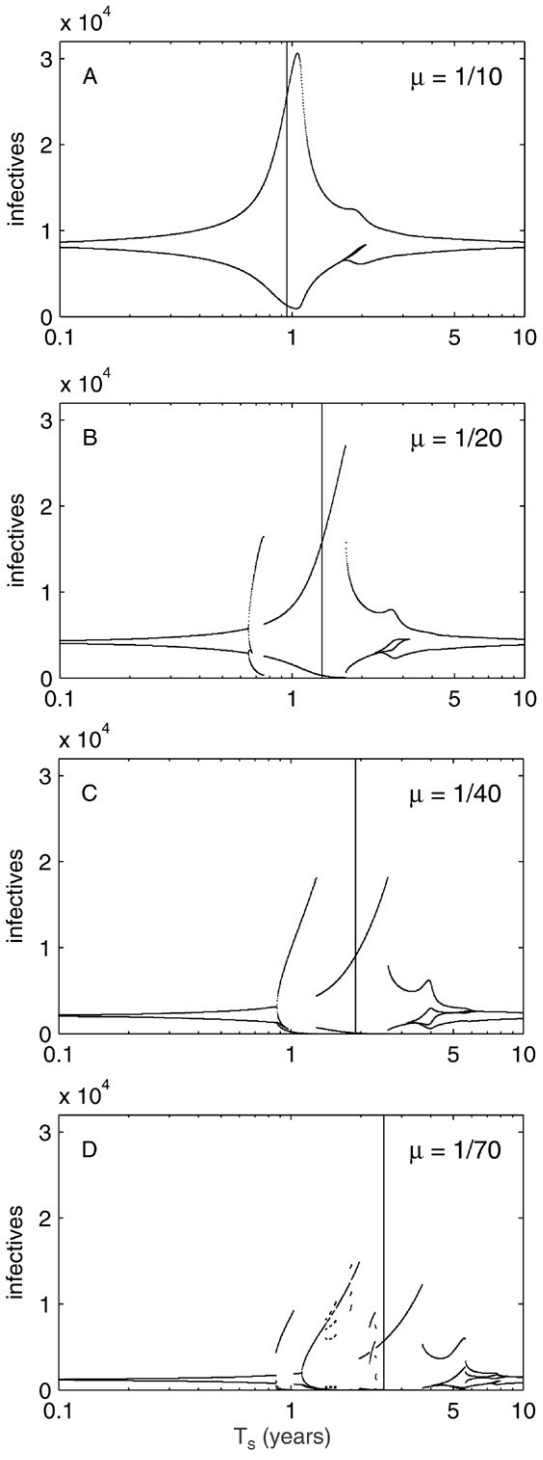

Fig. 1. Resonance diagrams showing the effect of seasonality in transmission. The peak and trough values of the number of infectives (as determined by Eqs. (1)–(4)) are plotted against the period T_S of the seasonal forcing modeled by Eq. (8). Parameter values are $N = 5 \times 10^6$ individuals, $\sigma^{-1} = 7.5$ days, $\gamma^{-1} = 6.5$ days, $\beta_0 = 0.0002$ yr$^{-1} \cdot$ individual^{-1}, and $\beta_1 = 0.1$, yielding a R_0 approximately equal to 17. The recruitment rate takes the following values: $\mu^{-1} = 10, 20, 40, 70$ yr for A, B, C, and D respectively. The attractors were determined from a 20-year period, after 180 years of transients were discarded. For each diagram, 1001 dynamics were simulated, regularly spaced on the decimal logarithm scale of the period. Initial conditions were $S = 0.05N$, $E = I = 0.0001N$. The vertical lines correspond to the estimation $\hat{T}$ of the inherent oscillatory periods T from the linear approximation of Eq. (7). Note the logarithm scale on the x-axes.

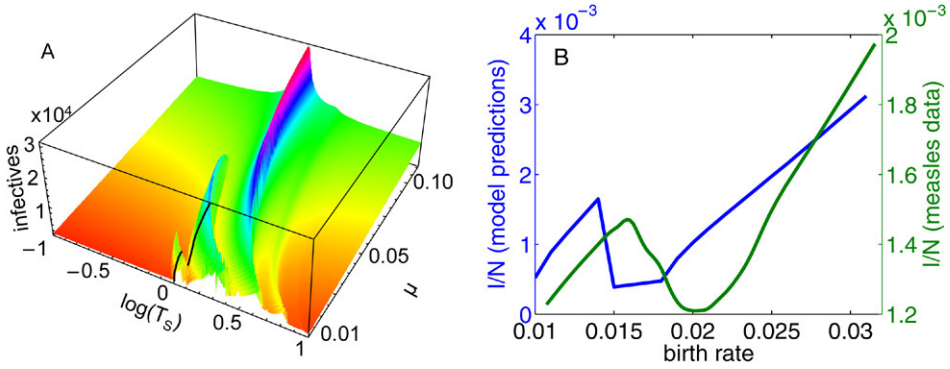

Fig. 2. A, Resonance diagram showing the effects of seasonality in transmission and nonlinearity. The peak values of the number of infectives (as determined by Eqs. (1)–(4)) are plotted against both the period T_S of the seasonal forcing modeled by Eq. (8) and the recruitment rate μ. The model is given by Eqs. (1)–(4) and (8). Initial conditions and parameter values are as in Fig. 1 except that μ varies from 0.01 to 0.1 yr^{-1} by steps of 0.001. The black line shows the values of the surface corresponding to measles parameters with $T_S = 1$ yr and μ varying from 0.01 to 0.035 yr^{-1}. B, Relationship between the maximum number of infectives and the birth rate in England and Wales in the pre-vaccine era (1944–1966). For each year from 1944 to 1966 the maximum number of infectives and the number of births were recorded. Both of these numbers were divided by the median city size between 1944 and 1966. The green curve corresponds to the smoothed values after a lowess regression with a tensor parameter equal to 2/3. The blue curve corresponds to the model prediction (black curve of A). (For interpretation of the references to colour in this figure legend, the reader is referred to the web version of this article.)

and Grossman [26] have reported a threshold effect for the seasonal forcing amplitude β_1 (see also, [44] and [46] for more rigorous mathematical proofs for the *SIR* and *SEIR* models, respectively). Another threshold effect is associated with the value of the baseline coefficient of transmission β_0 (or μ, recalling the aforementioned correspondence between μ and β_0). This is visible on Fig. 1: parametric resonance occurs around $T_S = 2$ yr in Fig. 1A and when μ decreases from Fig. 1A to D, the number of parametric peaks increases. This is even more apparent on Fig. 2A where the dependence of the resonance period on β_0 is responsible for the curvature observed on the figure. Note that this effect of β_0 is particularly pronounced for the biologically realistic values of μ ($0.01 < \mu < 0.05$) where the nonlinearity is high. The relation between the thresholds on β_1 and on β_0 is treated in [5]. Grossman [26] derived analytical formulations of the thresholds associated to each parametric resonance peak and showed a direct correlation between the aforementioned local stability of the system (defined by the $2A/T$ ratio) and its excitability, here defined by the threshold value on β_1 (see [44] and [46] for rigorous mathematical treatments). Subharmonic parametric resonance has been suggested to explain the biennial cycles of measles epidemics [35,47]. Moreover, Schwartz and Smith [44] and Smith [46] showed that several subharmonics of different periods can be simultaneously stable and further pointed out that random effects in the environment could perturb the state of the system from the domain of attraction of one subharmonic to that of another, producing aperiodic looking levels of incidence. This is greatly enhanced by the fact that the basins of attraction of the different subharmonics are largely intertwined [43,17].

3.5. Detection of resonance in measles data

Figs. 1 and 2A illustrate, in a general theoretical context, resonance phenomena for a given recruitment rate μ when T_S is varied. Because of the curvature observed in Fig. 2A, all the resonance phenomena described above are also observed for a given period T_S of the seasonal forcing when the recruitment rate μ is varied. This observation is practically relevant for the study of a particular disease since it implies that small variations in birth rate and/or vaccination coverage may dramatically change the severity of the epidemics and not necessarily in an intuitive manner. This generally echoes the findings of Dietz [15], who studied the effect of R_0 (see Eq. (5)) in an *SIR* framework with annual oscillations in the coefficient of transmission. We explored these predictions using weekly notification data for measles, and associated demographic data, for 60 towns and cities of England and Wales in the pre-vaccine era (1944–1966). See [9] for more details on the data set.

For measles parameter values, the model predicts parametric resonance in the dynamics: setting $T_S = 1$ yr in Fig. 2A and varying μ within a biologically meaningful region (i.e. from 0.01 to 0.035/person/yr), we observe a peak followed by an increase in the number of infectives (see the black line on Fig. 2A which is the same as the blue curve on Fig. 2B). We explored the data by calculating the maximum of the attractor and plotting it against the per capita birth rate, with the trend smoothed by a lowess regression (with a tensor parameter of 2/3). In practice, for each city, we truncated the measles case notification and birth time series in adjacent intervals of a fixed duration. On each of these intervals we considered the largest reported number of cases and the mean number of births. Both of these quantities were divided by the median city size between 1944 and 1966, producing our estimations of the maximum of the attractor and its corresponding per capita birth rate. Fig. 2B shows the results for a time interval of 1 year, though analyses for time intervals of 2, 3, and 4 years gave similar results. The observed patterns qualitatively fit model predictions rather well (compare the two curves in Fig. 2B). Quantitative discrepancy are certainly due to the simplicity of our model (in particular the sinusoidal form of the periodic forcing), and the difficulty to analyze such a dataset (the scale of birth rate variation is lower than the mean age at infection). Also, in the data set, the population sizes are assumed constant (and equal to the median city sizes between 1944 and 1966) which obviously is not the case. Such an approximation might also be responsible,

to some degree, for the discrepancy between model predictions and actual data. Therefore, these results highlight the fact that changes in the recruitment in susceptibles (either due to systematic trends in the crude birth rate or vaccination) not only have qualitative consequences through dynamical transitions but, due to resonance effects, may also have major quantitative consequences such as dramatic changes in the amplitude of the oscillations.

4. Pulse vaccination

4.1. Definition and theoretical background

The most commonly used strategy for control of infections such as measles is to immunize infants once they have reached a certain age (e.g. 12–25 months for the MMR vaccine in the USA). This process however requires a rather high vaccination coverage (around 95% for measles) for disease eradication to be achieved in practice. An alternative (and potentially less expensive) strategy is vaccination in pulses [2, 36]. This approach, based on theoretical results on population dynamics in varying environments [1], consists of vaccinating a proportion p of the susceptible population every T_V years. The essential aim is to antagonize (or entrain) natural dynamics by a different temporal process. This theory has been successfully applied in campaigns against poliomyelitis and measles in Central and South America and measles in the UK in 1994 (see references in [16]).

The theoretical challenge of pulse vaccination is the analytical determination (for specified values of p and μ) of the optimal value $T_V^{\max}$ which ensures the eradication of the disease. The rationale behind this, derived from the *SIR* model, is simply to repeatedly remove susceptibles in order to ensure that the proportion of susceptibles $S(t)/N$ remains consistently below the threshold $s_c = 1/R_0$ required for an increase in the number of infectives. This led to the approximation $T_V^{\max} = A$, where A is the mean age at infection [2]. Further detailed analyses revealed that to prevent an epidemic, it is sufficient that the mean value of $S(t)/N$, averaged over the pulsing period, remains below s_c. For an *SIR* model with constant coefficient of transmission, this led to the following relationship between $T_V^{\max}$ and p [45]:

$$T_V^{\max} = \frac{p\,\gamma}{\beta\mu(1 - p/2 - \gamma/\beta)}. \tag{11}$$

This value of $T_V^{\max}$ can be substantially larger than the mean age at infection A and remains a good approximation for the *SEIR* model, as long as β is constant [16]. When the transmission rate is periodic, β in Eq. (11) should be replaced by its mean value β_0 [45,16]. Once $T_V < T_V^{\max}$, the disease is thus expected to disappear. Should $T_V > T_V^{\max}$, however, the pulsed nature of this vaccination strategy may give rise to a rich variety of dynamics [45]. One important potential consequence is an increased likelihood in epidemic synchrony across sub-populations [18]. Another possible consequence of vaccination in pulses may be resonance effects associated with the frequency of vaccination events (as briefly mentioned by d'Onofrio [16]). We show here, via extensive numerical simulations, the conditions under which pulse vaccination can result in very large epidemics.

4.2. Investigating the resonance effect of pulse vaccination

A proportion p of the susceptible population is now vaccinated every T_V years and the following equation should be added to the previous model (Eqs. (1)–(4) and (8)):

$$S(kT_V^+) = (1 - p) \cdot S(kT_V^-), \quad k \in \mathbb{N} \tag{12}$$

where T_V^- and T_V^+ respectively refer to the instants that immediately precedes and follows the vaccination pulse. Given a vaccination proportion p and $T_V > T_V^{\max}$, two parameters may further influence the onset of resonance: the susceptible recruitment rate μ (or, equivalently, the mean coefficient of transmission β_0), and the amplitude of seasonality in transmission (β_1; Eq. (8)). In the previous section, we studied the resonance effects associated with the seasonal transmission. We are now interested in the resonance phenomenon arising from the periodic nature of vaccination pulses. We proceed step by step in order to distinguish the resonance effects due to pulse vaccination from those due to seasonal variations in transmission. First consider the model given by Eqs. (1)–(4), (8) and (12) with constant transmission (i.e. $\beta_1 = 0$ in Eq. (8)). In this setup, Fig. 3 shows resonance diagrams plotting the peak and trough values of the number of infectives against the logarithm of the period of vaccination T_V. To identify the influence of the system nonlinearities we proceed as before (c.f. Fig. 1) through variation in population turn-over rate μ, though the range of μ is smaller and more realistic in Fig. 3 than in Fig. 1. More precisely, Fig. 3D corresponds to the birth rate observed in western countries while Fig. 3A to that observed in some African countries.

Shulgin et al. [45] pointed out that when $T_V > T_V^{\max}$ the solution $I(t) = 0$ becomes unstable and the number of infectives begins to exhibit large amplitude oscillations. When T_V is further increased, a sequence of period doubling bifurcations interspersed with chaos is observed. Here, we further observe that a realistic increase in the recruitment rate μ from 0.02 (Fig. 3D) to 0.05 (Fig. 3A) reduces the chaotic region. A second effect of nonlinearity associated with the decrease of the population turn-over rate μ from Fig. 3A to Fig. 3D is the shift of the attractor towards the high values of the period of the forcing. This phenomenon has been already observed on Fig. 1 and is due to the above-mentioned increased dependency between the amplitude and the frequency of the oscillations when the level of nonlinearity increases [29]. For simplicity, we will focus our analysis on the structure of the attractor of a non-chaotic dynamics (Fig. 3A). Note however that the following observations are robust relative to the complexity level of the dynamics. This robustness appears when taking into account the temporal dimension which is not visible in the resonance diagrams of Fig. 3. Indeed, when we estimate the duration spent by the dynamics in each part of its chaotic attractor of Fig. 3D, we get a structure pretty close to that of Fig. 3A (results not shown).

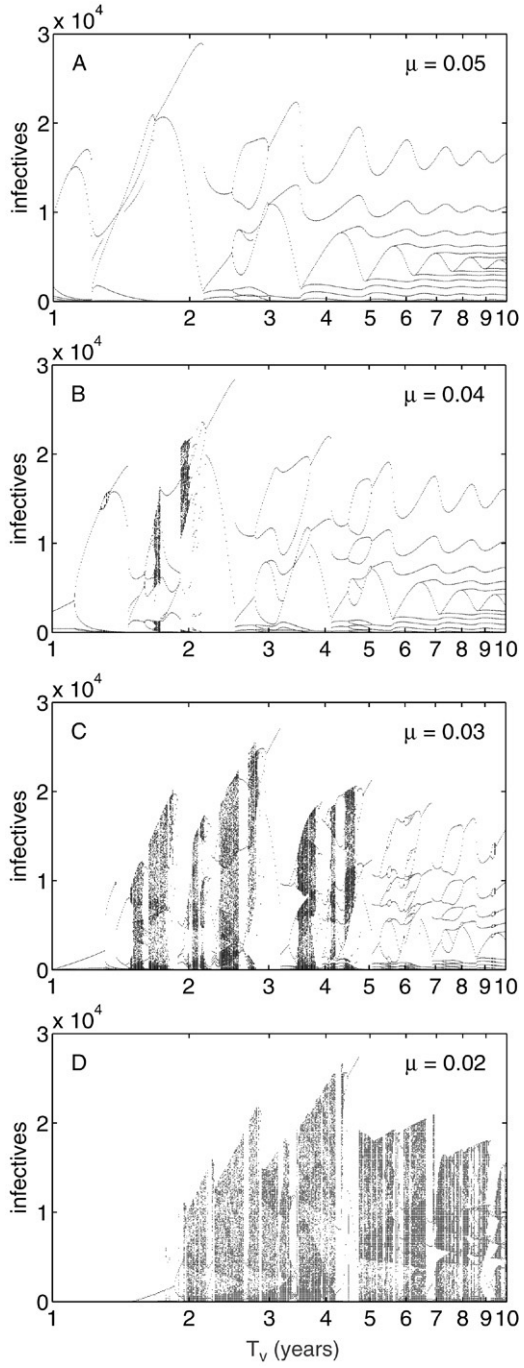

Fig. 3. Resonance diagrams showing the effect of pulse vaccination, ignoring seasonality in transmission. The peak and trough values of the number of infectives (as determined by Eqs. (1)–(4)) are plotted against the period T_V of the pulse vaccination modeled by Eq. (12). The attractors were determined from a period encompassing 200 vaccination events after the first 300 years and the initial 100 vaccination events were discarded. For each diagram, 501 dynamics were simulated, regularly spaced on the decimal logarithm scale of the period. Initial conditions were $S = 0.05N$, $E = I = 0.0001N$. Parameter values are the same as in Fig. 1 except that here $\beta_1 = 0$ and $T_V = 1$ yr in Eq. (8). The vaccination coverage $p = 0.4$ in Eq. (12) and the recruitment rate takes the following values: $\mu = 0.05, 0.04, 0.03, 0.02$ yr^{-1} for A, B, C, and D respectively. Note the logarithm scale on the x-axes.

The amplitude of the oscillations changes with T_V. All peaks occurring at a forcing period T_V greater than 2 are harmonics of the main resonance peak observed at $T_V \simeq 2$ yr. The bifurcations associated with each increase in the amplitude indicate instability and are characteristic of parametric resonance. As visible in Fig. 3A, the resonance phenomenon due to the periodic nature of this vaccination strategy may locally give rise to unexpected increases in the epidemic peaks as the frequency $1/T_V$ of vaccination increases. Moreover, increases in the peaks tend to be associated with deeper troughs (not shown) which thus may increase the probability of disease extinction in the case of small populations. More importantly, the duration of the epidemic is also influenced (see below).

4.3. Introducing seasonality to pulse vaccination's resonance

Consider now the case where transmission is seasonal (i.e. $\beta_1 > 0$ in Eq. (8)), with a fixed period T_S equal to 1 yr. In practice, two β_1 values ($\beta_1 = 0.01$ and $\beta_1 = 0.10$) have been added to the dynamics described in Fig. 3A (where β_1 had been set to zero). In both seasonality cases, our simulations tracked how four critical quantities behave when T_V varies: the amplitude of infectives (Fig. 4A, B), the cumulative number of cases (Fig. 4C, D), the mean annual number of infectives (Fig. 4E, F), and the number of vaccinated individuals (Fig. 4G, H). Clearly, increasing β_1 from 0 (Fig. 3A) to 0.01 (Fig. 4A) or the more realistic value [17] of 0.10 (Fig. 4B) increases variation in the dynamics of infectives, eventually leading to chaos. Note however that the general structure of the resonance peaks is not affected by the level of complexity that may be present in the dynamics. Indeed, the confusing patterns obtained when $\beta_1 = 0.10$ (Fig. 4B) resemble those obtained for $\beta_1 = 0.01$ (Fig. 4A) and for $\beta_1 = 0$ (Fig. 3A).

The two levels of seasonality ($\beta_1 = 0.01$ and $\beta_1 = 0.10$) also differentially affect the instantaneous number of new infectives (Fig. 4C, D). Here the number tracked corresponds to the individuals entering the infectious compartment between two vaccination pulses, scaled by the between-vaccination duration: $(1/T_V)\int_{kT_V}^{(k+1)T_V} \sigma E(t)\mathrm{d}t$. Whatever the value of β_1, the peaks in incidence (Fig. 4C, D) are associated with those observed in the resonance diagrams (Fig. 4A, B). When $\beta_1 = 0.10$ it remains visible: incidence exhibits a sudden change at $T_V \simeq 2$ years (Fig. 4D), which precisely coincides with the main peak on the resonance diagram (Fig. 4B).

More relevant from an epidemiological point of view may be the mean annual number of infectives. Its variation with T_V is shown in Fig. 4E, F. Here the mean considered was computed over a period encompassing 200 vaccination events, which has the advantage of smoothing the irregularities due to the complexity of the dynamics. Despite the general increase in the mean annual prevalence with T_V, these two plots clearly exhibit peaks wherever parametric resonance is observed in the resonance diagram (compare Fig. 4A, B with Fig. 4E, F). As expected, the observed pattern is even more clear-cut when the number of people actually vaccinated remains fixed as T_V varies (not shown). Practically, these resonance phenomena mean, somewhat counter-intuitively, that the mean annual number of infectives may locally (i.e. on the resonance domain) increase when T_V decreases. For example, in Fig. 4F, vaccination every 24 months yields a mean annual number

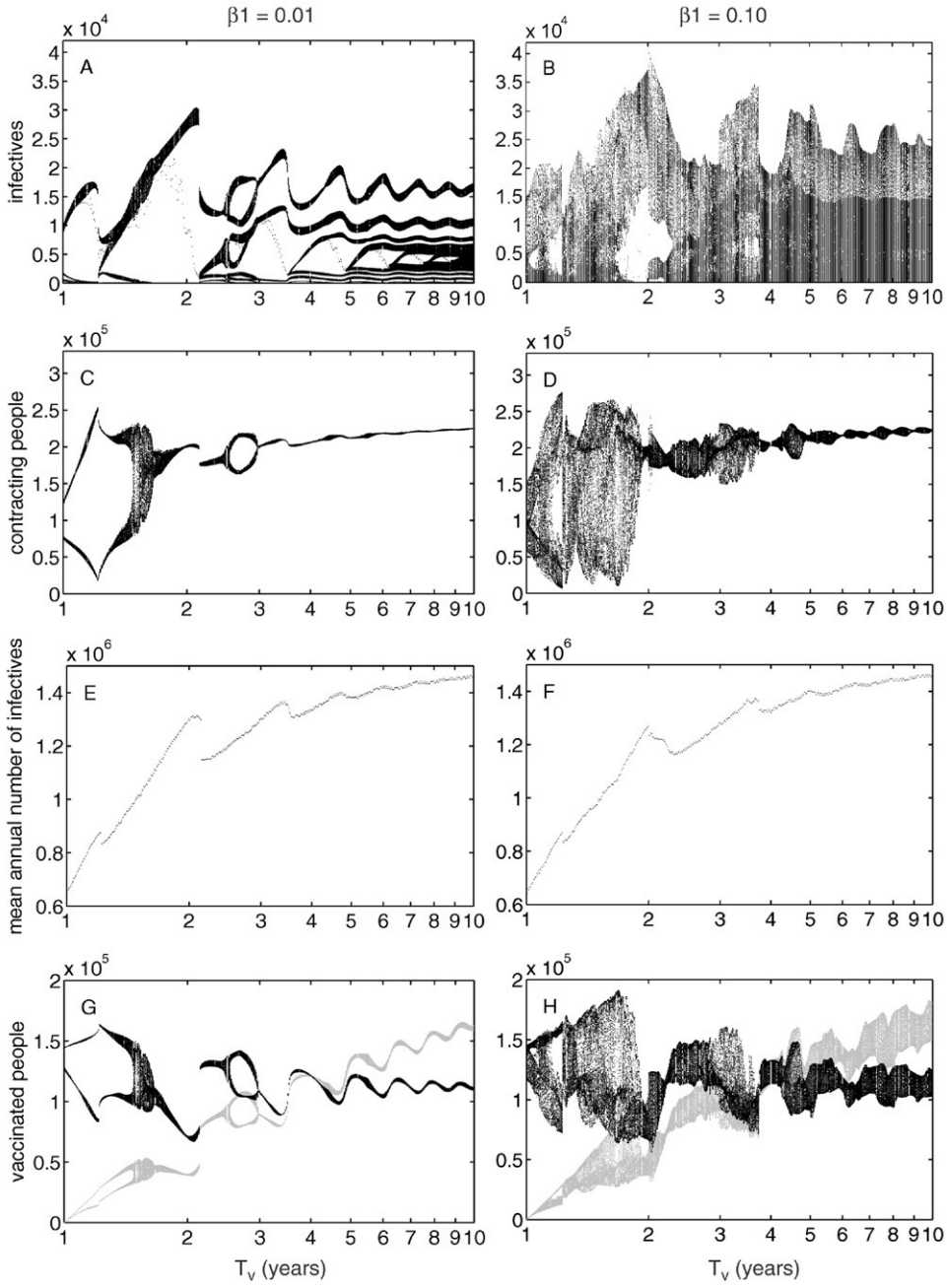

Fig. 4. Mixing seasonality and pulse vaccination. Dynamics of the model given by Eqs. (1)–(4) with an oscillating coefficient of transmission modeled by Eq. (8) and pulse vaccination modeled by Eq. (12). As in Fig. 3A, $\mu = 0.05\ \mathrm{yr}^{-1}$ and $p = 0.4$ in Eq. (12). In addition, $T_V = 1$ yr in Eq. (8). Seasonality is then introduced with $\beta_1 = 0.01$ (left column) and $\beta_1 = 0.10$ (right column). Each row shows the behavior of four critical quantities when T_V varies. A, B, resonance diagrams of the number of infectives. C, D, instantaneous number of people who get diseased between two vaccination pulses. This number is calculated by $(1/T_V)\int_{kT_V}^{(k+1)T_V} \sigma E(t)\mathrm{d}t$ (see text). E, F, Mean annual number of infectives. This is calculated on the period encompassing the last 200 events of vaccination. G, H, actual number of vaccinated people in the simulations (in black) and, in grey, the optimal number, as estimated by d'Onofrio [16]. The effective number is simply $p \cdot S(kT_V^-)$. The optimal estimation is $p_{\min} \cdot S(kT_V^-)$ where $p_{\min}$ is calculated from Eq. (11) and $k \in \mathbb{N}$. Initial conditions were $S = 0.05N$, $E = I = 0.0001N$. Note the logarithm scale on the x-axes.

of infectives (1275,000) that is 10% higher than vaccination every 28 months (1155,000). As β_1 decreases, this difference becomes even more pronounced: in Fig. 4E, vaccination every 25 months yields a mean annual number of infectives equal to 1315,000 which is 15% higher than a vaccination every 26 months which yields a mean annual number of infectives equal to 1145,000. The reason of this paradox is that, by its periodic nature, the pulse vaccination strategy make the recruitment rate in pace with the intrinsic dynamics of the disease, thus optimizing its transmission.

Finally, let's focus on the number of people effectively vaccinated and its variation with β_1 and T_V (in black in Fig. 4G, H). This number is simply calculated from $p \cdot S(kT_V^-)$, $k \in \mathbb{N}$. Fig. 4G, H also show in grey the minimum number of people

to vaccinate to theoretically reach eradication according to Shulgin et al. [45] and d'Onofrio [16]. This is calculated from $p_{\min} \cdot S(kT_V^-)$, $k \in \mathbb{N}$, where $p_{\min}$ is derived from Eq. (11) [45,16]. When $T_V < 2$ yr we observe on Fig. 4G, H that the number of people actually vaccinated in higher than the minimum required to theoretically reach eradication. However, instead of reaching disease eradication as expected, we still observe disease persistence (see corresponding Fig. 4A–F). Eq. (11) was derived neglecting the effect of the amplitude β_1 of the seasonal transmission (see Eq. (8)) on the value of $T_V^{\max}$ [45, 16]. Our numerical results suggest that, for realistic parameter values, neglecting the effect of the amplitude of the seasonal transmission can lead to somewhat overoptimistic high values of the optimal pulse period $T_V^{\max}$.

5. Discussion

Epidemiological systems describing strongly immunizing infections are inherently oscillatory and thus are expected to produce resonance phenomena when undergoing periodic forcing [29]. For childhood diseases, one obvious mechanism for forcing is the seasonal variation in transmission due to the alternation of holidays and school terms [35,20,42,21,4]. A second cause of external forcing is associated with the periodic nature of pulse vaccination (when the vaccination coverage and/or the pulse frequency are not high enough to eradicate the disease; [16]). In this study, we have numerically explored the dynamical effects of resonance, especially within the context of pulse vaccination.

We first considered the simple *SEIR* model with a sinusoidal coefficient of transmission. Here, the source of nonlinearity is the density-dependent transmission process and the strength of nonlinearity increases as the population turn-over rate μ decreases or, equivalently, when the mean coefficient of transmission β_0 decreases [17]. Resonance diagrams with the period T_S of the seasonal forcing as the control parameter show the existence of two kinds of resonance: harmonic and parametric, depending on the strength of nonlinearity. Harmonic resonance is characterized by a single high peak in the amplitude of epidemics and occurs when $T_S \simeq T$, with T the natural period of the system in the absence of forcing. Parametric resonance is an instability phenomenon and is characterized by a series of small peaks in the amplitude of epidemics. These peaks occur at integer fractions of the natural period T. The appearance of each parametric resonance peak occurs at a threshold value on the level of nonlinearity (as determined by, for example, the population turn-over rate μ) and the values of these thresholds depend on the amplitude β_1 of the seasonal forcing. The curvature observed on Fig. 2A is responsible for the fact that the effect of resonance may be also detected when the level of nonlinearity varies, for a fixed period of the seasonal forcing. This prediction has been successfully verified on real data of measles cases from England and Wales in the pre-vaccine era.

In a similar way, we investigated the potential for resonance associated with the periodic nature of pulse vaccination. For simplicity, we began by considering pulse vaccination in the absence of seasonality in transmission. We clearly detected parametric resonance, which results in higher peaks and deeper troughs in infective numbers. Obviously, deeper troughs may increase the probability of disease extinction, especially in small populations. However, the effects of resonance are substantially more dramatic on the peaks than the troughs (Fig. 3). Moreover, we found an unexpected local (in terms of vaccination frequency) increase in the number of infectives as vaccination pulses become more frequent. This finding holds even when the threshold vaccination level required for eradication in the absence of seasonality is exceeded. From then, we added seasonal variation in transmission. Our simulations show that the inclusion of seasonality has little impact on the system behavior (including the structure of the resonance peaks) other than to force the oscillations into a chaotic mode. For simplicity, the effects of resonance were investigated on situations where the dynamics behave relatively simply (i.e. high population turn-over rate μ, high mean coefficient of transmission β_0, and low amplitude β_1 on the coefficient of transmission). Nevertheless, our conclusions were robust relative to the level of complexity in the dynamics and remained unchanged when considering realistic μ, β_0, and β_1 values.

The results outlined in the paper have public health implications pertaining to pulse vaccination strategies. The classical mass vaccination scheme is based on the static properties of the host–disease system. What makes the recently developed pulse vaccination theory potentially more efficient is that it explicitly accounts for the dynamics of the host population through the influx of susceptibles (via births). Substantial progress has been made in determining the optimal vaccine coverage p and pulsing frequency T_V in different epidemiological contexts [2,36,45,48,16]. However, our numerical results warn that neglecting the effect of the amplitude β_1 of the seasonal transmission on the optimal pulse period $T_V^{\max}$ ([45,16]; see Eq. (11)) can be an overoptimistic approximation which can have dramatic consequences in practice in not leading the disease to extinction as expected.

We have also shown that the interference between intrinsic diseases dynamics and the periodic nature of an imperfect pulse vaccination scheme may produce unexpected results, such as an increase in the number of infectives with the frequency of vaccination. As a consequence, further refinements of the pulse vaccination strategy need to take seasonal disease dynamics into full account. From a theoretical perspective, there is thus a need for the development of analytical epidemiological models that incorporate information such as the natural period of the disease in question. From a practical point of view, we may adopt a more ad hoc approach. In other words, the design of a pulse vaccination policy on a particular epidemiological system should be preceded by the determination of the disease dynamics characteristics and its resonance domain. Simulation models will be of great help for such tasks.

Acknowledgments

We would like to thank Alberto d'Onofrio for his comments and advice which greatly improved the first versions of the

manuscript, and Sylvain Gandon for useful discussions, and suggestions. Christine Chevillon brought invaluable comments on the last versions of the manuscript. MC is funded by a BDI CNRS/Région Languedoc-Roussillon, PR is supported by the Ellison Medical Foundation, the National Institutes of Health and the National Science Foundation. JFG is sponsored by IRD and CNRS.

References

[1] Z. Agur, Randomness synchrony population persistence, J. Theoret. Biol. 112 (1985) 677–693.
[2] Z. Agur, L. Cojocaru, R.M. Anderson, Y.L. Danon, Pulse mass measles vaccination across age cohorts, Proc. Natl. Acad. Sci. USA 90 (1993) 11698–11702.
[3] R.M. Anderson, B.T. Grenfell, R.M. May, Oscillatory fluctuations in the incidence of infectious disease and the impact of vaccination: time series analysis, J. Hyg. Camb. 93 (1984) 587–608.
[4] R.M. Anderson, R.M. May, Infectious Diseases of Humans: Dynamics and Control, Oxford University Press, Oxford, 1991.
[5] J. Aron, I. Schwartz, Seasonality and period-doubling bifurcations in an epidemic model, J. Theoret. Biol. 110 (1984) 665–679.
[6] N.T.J. Bailey, The Mathematical Theory of Infectious Diseases, Charles Griffin and Company Ltd, London, 1975.
[7] M.S. Bartlett, Measles periodicity and community size, J. Roy. Statist. Soc. Ser. A 120 (1957) 48–70.
[8] L. Billings, I.B. Schwartz, Exciting chaos with noise: unexpected dynamics in epidemic outbreaks, J. Math. Biol. 44 (2002) 31–48.
[9] O.N. Bjørnstad, B. Finkenstädt, B.T. Grenfell, Dynamics of measles epidemics: estimating scaling of transmission rates using a time series SIR model, Ecol. Monogr. 72 (2002) 169–184.
[10] B.M. Bolker, B.T. Grenfell, Chaos and biological complexity in measles dynamics, Proc. R. Soc. Lond. B 251 (1993) 75–81.
[11] B.M. Bolker, B.T. Grenfell, Space, persistence and dynamics of measles epidemics, Philos. Trans. R. Soc. Lond. B 348 (1995) 309–320.
[12] B.M. Bolker, B.T. Grenfell, Impact of vaccination on the spatial correlation and persistence of measles dynamics, Proc. Natl. Acad. Sci. USA 93 (1996) 12648–12653.
[13] S. Deguen, A. Flahault, Impact of immunization of seasonal cycle of chickenpox, Eur. J. Epidemiol. 16 (2000) 1177–1181.
[14] O. Diekmann, J.A.P. Heesterbeek, Mathematical Epidemiology of Infectious Diseases: Model Building, Analysis and Interpretation, John Wiley & Sons, Chichester, 2000.
[15] K. Dietz, The incidence of infectious diseases under the influence of seasonal fluctuations, Lect. Notes Biomath. 11 (1976) 1–5.
[16] A. d'Onofrio, Stability properties of pulses vaccination strategy in SEIR epidemic model, Math. Biosci. 179 (2002) 57–72.
[17] D.J.D. Earn, P. Rohani, B.M. Bolker, B.T. Grenfell, A simple model for complex dynamical transitions in epidemics, Science 287 (2000) 667–670.
[18] D.J.D. Earn, P. Rohani, B.T. Grenfell, Persistence, chaos and synchrony in ecology and epidemiology, Proc. R. Soc. Lond. B 265 (1998) 7–10.
[19] S. Ellner, B.A. Bailey, G.V. Bobashev, A.R. Gallant, B.T. Grenfell, D.W. Nychka, Noise and nonlinearity in measles epidemics: combining mechanistic and statistical approaches to population modeling, Am. Nat. 151 (1998) 425–440.
[20] P.E.M. Fine, J.A. Clarkson, Measles in England and Wales. 1. An analysis of factors underlying seasonal patterns, Int. J. Epidemiol. 11 (1982) 5–14.
[21] P.E.M. Fine, J.A. Clarkson, Seasonal influences on pertussis, Int. J. Epidemiol. 15 (1986) 237–247.
[22] P. Glendinning, L.P. Perry, Melnikov analysis of chaos in a simple epidemiological model, J. Math. Biol. 35 (1997) 359–373.
[23] J. Greenman, M. Kamo, M. Boots, External forcing of ecological and epidemiological systems: a resonance approach, Physica D 190 (2004) 136–151.
[24] B.T. Grenfell, O.N. Bjørnstad, B.F. Finkenstädt, Dynamics of measles epidemics: scaling noise, determinism, and predictability with the TSIR model, Ecol. Monogr. 72 (2002) 185–202.
[25] B.T. Grenfell, O.N. Bjørnstad, J. Kappey, Travelling waves and spatial hierarchies in measles epidemics, Nature 414 (2001) 716–723.
[26] Z. Grossman, Oscillatory phenomena in a model of infectious diseases, Theor. Popul. Biol. 18 (1980) 204–243.
[27] Z. Grossman, I. Gumowski, K. Dietz, The incidence of infectious diseases under the influence of seasonal fluctuations — analytical approach, in: V. Lakshmikantham (Ed.), Nonlinear Systems and Applications, Academic Press, New York, 1977, pp. 525–546.
[28] H.W. Hethcote, Oscillations in an endemic model for pertussis, Can. Appl. Math. Q. 6 (1998) 61–88.
[29] E.A. Jackson, Perspectives of Nonlinear Dynamics: Volume 1, Cambridge University Press, Cambridge, 1992.
[30] D.W. Jordan, P. Smith, Nonlinear Ordinary Differential Equations, Oxford University Press, Oxford, 1999.
[31] M.J. Keeling, B.T. Grenfell, Disease extinction and community size: modeling the persistence of measles, Science 275 (1997) 65–67.
[32] M.J. Keeling, P. Rohani, B.T. Grenfell, Seasonally forced disease dynamics explored as switching between attractors, Physica D 148 (2001) 317–335.
[33] W.O. Kermack, A.G. McKendrick, A contribution to the mathematical theory of epidemics, Proc. R. Soc. Lond. A 115 (1927) 700–721.
[34] A.L. Lloyd, R.M. May, Spatial heterogeneity in epidemic models, J. Theoret. Biol. 179 (1996) 1–11.
[35] W.P. London, J.A. Yorke, Recurrent outbreaks of measles, chickenpox and mumps. I. Seasonal variation in contact rates, Am. J. Epidemiol. 98 (1973) 453–468.
[36] D.J. Nokes, J. Swinton, Vaccination in pulses: a strategy for global eradication of measles and polio? Trends Microbiol. 5 (1997) 14–19.
[37] C.J. Rhodes, H.J. Jensen, R.M. Anderson, On the critical behaviour of simple epidemics, Proc. R. Soc. Lond. B 264 (1997) 1639–1646.
[38] P. Rohani, D.J.D. Earn, B.T. Grenfell, Opposite patterns of synchrony in sympatric disease metapopulations, Science 286 (1999) 968–971.
[39] P. Rohani, D.J.D. Earn, B.T. Grenfell, Impact of immunisation on pertussis transmission in England and Wales, Lancet 355 (2000) 285–286.
[40] P. Rohani, M.J. Keeling, B.T. Grenfell, The interplay between determinism and stochasticity in childhood diseases, Am. Nat. 159 (2002) 469–481.
[41] W.M. Schaffer, M. Kot, Nearly one dimensional dynamics in an epidemic, J. Theoret. Biol. 112 (1985) 403–427.
[42] D. Schenzle, An age-structured model of pre- and post-vaccination measles transmission, IMA J. Math. Appl. Med. Biol. 1 (1984) 169–191.
[43] I. Schwartz, Multiple stable recurrent outbreaks and predictability in seasonally forced nonlinear epidemic models, J. Math. Biol. 21 (1985) 347–361.
[44] I. Schwartz, H. Smith, Infinite subharmonic bifurcation in an SEIR epidemic model, J. Math. Biol. 18 (1983) 233–253.
[45] B. Shulgin, L. Stone, Z. Agur, Pulse vaccination strategy in the SIR epidemic model, Bull. Math. Biol. 60 (1998) 1123–1148.
[46] H. Smith, Multiple stable subharmonics for a periodic epidemic model, J. Math. Biol. 17 (1983) 179–190.
[47] D. Stirzaker, A perturbation method for the stochastic recurrent epidemic, J. Inst. Math. Appl. 15 (1975) 135–160.
[48] L. Stone, B. Shulgin, Z. Agur, Theoretical examination of the pulse vaccination policy in the SIR epidemic model, Math. Comput. Modeling 31 (2000) 207–215.
[49] C.W. Tidd, L.F. Olsen, W.M. Schaffer, The case for chaos in childhood epidemics. II. Predicting historical epidemics from mathematical models, Proc. R. Soc. Lond. B 254 (1993) 257–273.
[50] H.C. Tuckwell, L. Toubiana, J.-F. Vibert, Enhancement of epidemic spread by noise and stochastic resonance in spatial network models with viral dynamics, Phys. Rev. E 61 (2000) 5611–5619.